

# On the axisymmetric thin disk model of flattened galaxies

Łukasz Bratek<sup>1</sup>, Joanna Jałocha<sup>1</sup> and Marek Kutschera<sup>1,2</sup>

<sup>1</sup> *H. Niewodniczański Institute of Nuclear Physics, Polish Academy of Sciences, Radzikowskiego 142, 31-342 Kraków, Poland*

<sup>2</sup> *M. Smoluchowski Institute of Physics, Jagellonian University, Reymonta 4, 30-059 Kraków, Poland*

## ABSTRACT

Non-monotonic features of rotation curves, and also the related gravitational effects typical of thin disks – like backward-reaction or amplification of rotation by negative surface density gradients – which are characteristic imprints of disk-like mass distributions, are discussed in the axisymmetric thin disk model. The influence of the data cutoff in rotational velocity measurements on the determination of the mass distribution in flattened galaxies is studied.

It has also been found that the baryonic matter distribution in the spiral galaxy NGC 5475, obtained in the axisymmetric thin disk approximation, accounts for the rotation curve of the galaxy. To obtain these results, the iteration method developed recently by the authors has been applied.

**Key words:** gravitation: disk model, galaxies: kinematics and dynamics, individual: NGC 5475, mass function

## 1 INTRODUCTION

The analysis of rotation curves provides the most reliable means for ascertaining at least the gross distribution of gravitating matter within spiral galaxies, as Alar Toomre pointed out (Toomre 1963). In the same paper Toomre formulated a complete mathematical model of an axisymmetric and infinitely thin disk rotating under its own gravity. The model offers a tool for determining the equilibrium mass distribution directly from the rotation law of a highly flattened system, such as a spiral galaxy. It is assumed in the framework of the model, that orbits of stars, gas, etc., are circular, and that gravitational forces are balanced solely by centrifugal forces; the effect of pressure is thus ignored. A few years earlier, following the work reported by (Burbidge et al. 1959), Brandt discussed less general situation of a very flattened system regarded as an assembly of osculating homoeoids compressed to a circular disk (Brandt 1960). All these papers followed many other pioneering ones referred to in (Brandt 1960).

The customary parametric few-component models relate the mass distribution of baryonic matter mainly to luminosity measurements. The obtained amount of luminous mass is usually insufficient to account for the observed rotation of galaxies and a massive spherical dark halo is introduced as a remedy for the missing mass. The thin disk model with the surface mass density reconstructed mainly from rotation curves performs very well with strongly non-monotonic rotation curves, whereas the customary models have difficulties in explaining them. The thin disk model can easily account for high local gradients of rotational velocity, typically giving a lower total mass. In an extreme example,

the rotational velocity of an outer galactic region, falling off faster than Keplerian, cannot be explained by the presence of a massive spherically symmetric halo. However, such a feature may be explained using a flattened mass distribution with a suitably changing mass profile.

The major difficulty in the practical use of the disk model lies with unambiguous mass density reconstruction. Unlike for spherical symmetry, the density depends on the assumed extrapolation of the rotation curve beyond the last measurement point (referred to in this paper as the 'cutoff radius'). This is a consequence of the nonlocal relation between the surface density and the rotational velocity of a disk-like system. For a reliable reconstruction of the disk surface density, the rotation curve has to be known globally (which, for observational reasons, is impossible) or at least out to its Keplerian falloff.<sup>1</sup> Therefore, the velocity measurements must be supplemented with independent data in order to constrain the sought mass distribution. This may be achieved, for example, by taking into account the amount of hydrogen measured in the outermost galactic regions as was done in (Jałocha et al. 2008).

Mass estimates of spiral galaxies are strongly model-dependent. Rotational velocities, when interpreted in a spherical dark halo model, may greatly overestimate galactic masses as compared to the disk model. It is thus important to consider a phenomenologically acceptable model that gives a lower limit to the mass. The thin disk model may serve as such a reference model.

<sup>1</sup> Sofue & Rubin (2001) report on galaxies with Keplerian rotation curves at large radii

NGC 4736 is an example of a spiral galaxy with a rotation curve of which outer parts cannot be satisfactorily reconstructed when a spherical halo is assumed. By a simple examination one finds that in the circular orbit approximation, the rotation curve of this galaxy cannot be created by a spherical matter distribution. By applying the thin disk model, with no constraining assumptions about the mass-to-light ratio profile, one can find a mass profile in this galaxy that perfectly conforms with its rotation curve, and agrees with the amount of hydrogen observed at large radii, beyond the cutoff radius (Jałocha et al. 2008). Only insignificant (if any) amount of dark matter is required, whereas the customary models predict the galaxy to be dark matter dominated. In this paper we report also on another spiral galaxy, NGC 5457, in which the amount of baryonic matter found in the disk model accounts for this galaxy rotation.

### 1.1 The global thin disk model as a means of relating the rotation law to a mass distribution

The main objection against the use of the axisymmetric thin disk as a model of a spiral galaxy, is its instability with too short time scale (Toomre 1964; Ostriker & Peebles 1973). The simplest way to stabilize such a system is to add a sufficiently strong spherically symmetric potential. This is usually done by introducing a massive spherical halo of dark matter, which is believed to surround spiral galaxies. However, it should be noted that the galactic interior, irrespectively of its structure, produces at radii sufficiently large almost spherically symmetric potential that may stabilize the external circular orbits.

Putting the stability issue aside, the disk model is still useful for approximate description of the gravitational field of a flattened galaxy. Suppose that the rotation curve of such a galaxy represents the velocity of the streaming motion of matter rotating on roughly circular orbits in the galactic disk. The disk model associates with this rotation curve a formal surface mass density that may be considered as an approximation of the column density of matter in this galaxy. To ensure its applicability, we use the model only for describing galaxies with rotation curves breaking the condition of spherical mass distribution at large distances from their centers. We assume that this non-sphericity can be attributed to flattening of these galaxies. In these regions we therefore expect the disk model to better reflect the oblateness of such galaxies than the models with massive spherical halo. What's more, the customary rotation curve modeling already assumes a resultant thin disk surface density as a superposition of the stellar disk component's surface density and of the column density of the spherical bulge component projected onto the thin disk's plane. Based on these premises the use of the single global thin disk for modeling the whole mass distribution in a flattened galaxy seems justified. The only new qualitative thing is that the effective disk becomes extended further out to the outer part in the case when the sphericity condition is broken there, that is, when the massive spherical halo cannot be introduced.

## 2 THE SPHERICITY PROBLEM

The velocity of test bodies moving on circular orbits in the equatorial plane of a spherically symmetric mass distribution with a mass function  $M(r)$  is given by  $v(r) = \sqrt{GM(r)/r}$ . By analogy with this relation we define the Keplerian mass function  $r v^2(r)/G$  of a galaxy with a rotation curve  $v(r)$ . For a galaxy with a massive spherical CDM halo, the Keplerian mass function, at least for large radii, should agree with the true mass function of the galaxy.

Keplerian mass functions of some spiral galaxies decline or are non-monotonic in their outer parts, suggesting the presence of an extended, flattened and massive subsystem in these galaxies rather than a spherical one. The spherical dark halo may be excluded in favor of a large flattened subsystem if the sphericity condition –

$$\text{for all } r : (r v^2(r))' \geq 0 \quad (1)$$

– is broken at larger radii (beyond the central bulge). In this case the global disk model seems more appropriate for reconstruction of the mass distribution. Note, that the central spherical bulge may be represented by a column mass density in the disk plane since the details of the internal mass distribution are not very important for the determination of the gravitational field in the distant regions, thus the use of the disk model in the central regions is also acceptable.

Since there are many examples of disk-like mass configurations with their rotation laws satisfying the sphericity condition (1), violation of the condition at larger radii provides a strong argument for the presence of an extended flattened component and against a significant spherical halo. For example, the Toomre thin disk of unit mass with the surface mass density  $\sigma(x) = (1 + x^2)^{-3/2} / (2\pi)$  ( $x$  is a dimensionless radius in cylindrical coordinates), rotates differentially with velocity  $v(x) = x(1 + x^2)^{-3/4}$  (Toomre 1963), hence  $(xv^2(x))' = 3x^2(1 + x^2)^{-5/2} > 0$ . As so, a spherically symmetric mass distribution is possible with the same rotation curve. In the approximation of circular orbits, the sphericity condition is thus necessary, although not sufficient, for the presence of an extended and dominating spherical halo. Figure 1 shows two rotation curves that break inequality (1) at large radii.

## 3 ROTATION IN THE GRAVITATIONAL FIELD OF AN AXISYMMETRIC FLAT DISK

### 3.1 Basic equations

Rotational velocity  $v(\rho)$  of circular motion of a test body around the symmetry axis and in the symmetry plane of the gravitational field of an axisymmetric thin disk is related to the disk's surface mass density  $\sigma(\rho)$  by

$$\frac{v^2(\rho)}{4G\rho} = \mathcal{P} \left[ \int_0^\rho \sigma(\chi) \frac{\chi E\left(\frac{\chi}{\rho}\right)}{\rho^2 - \chi^2} d\chi - \int_\rho^\infty \sigma(\chi) \left( \frac{\chi^2 E\left(\frac{\rho}{\chi}\right)}{\rho(\chi^2 - \rho^2)} - \frac{K\left(\frac{\rho}{\chi}\right)}{\rho} \right) d\chi \right], \quad (2)$$

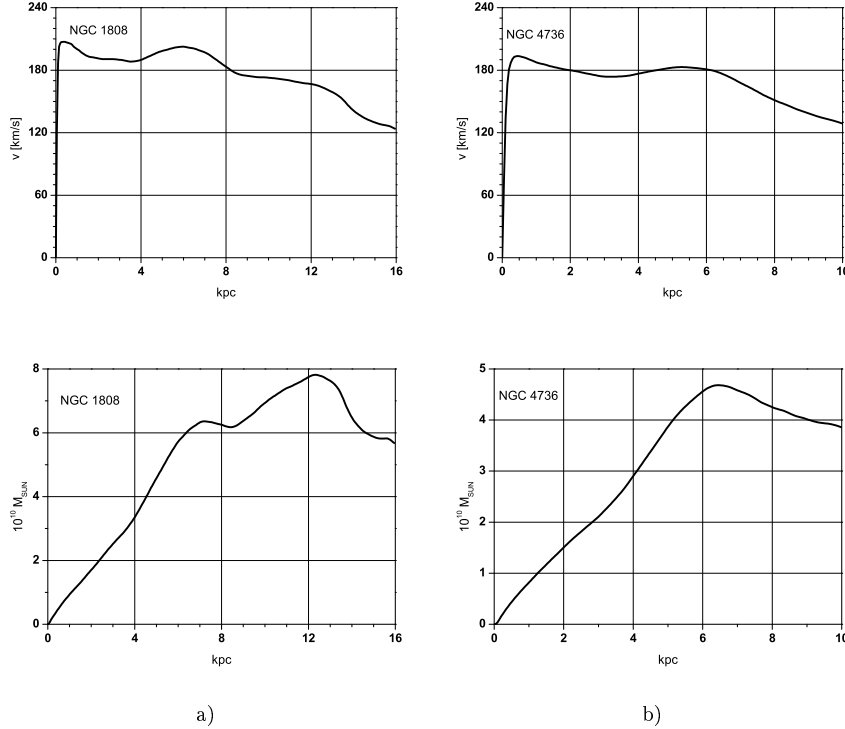


**Figure 1.** The upper plots show rotation curves of spiral galaxies **a)** NGC1808 and **b)** NGC4736. The lower plots show the corresponding Keplerian mass functions defined in the text. The unusual behavior of these functions (a mass function should be nondecreasing) suggests that matter distribution in these galaxies may be dominated by an extended and flattened galactic subsystem.

see appendix A.<sup>2</sup> The above integral exists in the 'principal value' sense, hence the  $\mathcal{P}$  symbol. The second part of the integral describes the backward interaction effect typical for disks – the velocity of rotation on a circular orbit is influenced also by matter present outside the orbit. Gravitation of disks is therefore qualitatively different from that of spherically symmetric systems. Note, that for arbitrary  $\sigma > 0$ , integral (2) may attain negative values at some radii. For such radii circular orbits are impossible.

The formal inverse of (2) reads

$$\sigma(\rho) = \frac{1}{\pi^2 G} \mathcal{P} \left[ \int_0^\rho v^2(\chi) \left( \frac{K\left(\frac{\chi}{\rho}\right)}{\rho \chi} - \frac{\rho}{\chi} \frac{E\left(\frac{\chi}{\rho}\right)}{\rho^2 - \chi^2} \right) d\chi + \int_\rho^\infty v^2(\chi) \frac{E\left(\frac{\rho}{\chi}\right)}{\chi^2 - \rho^2} d\chi \right]. \quad (3)$$

This integral exists if  $\lim_{\rho \rightarrow 0} \rho v(\rho) = 0$ , however in its derivation more stringent assumptions were imposed on  $v(\rho)$  (see appendix A).

<sup>2</sup>  $\rho$  is the radial variable in cylindrical coordinates and  $K$  and  $E$  are complete elliptic functions of the first and second kind, (Ryzhik & Gradstein 1951)

$$K(\kappa) = \int_0^{\pi/2} \frac{d\phi}{\sqrt{1 - \kappa^2 \sin^2 \phi}}, \quad E(\kappa) = \int_0^{\pi/2} d\phi \sqrt{1 - \kappa^2 \sin^2 \phi}$$

In the approximation of cold, circular streaming motion, relation (3) may be regarded as the definition of an effective surface mass density corresponding to the rotation curve of a flattened disk-like galaxy. However, the answer to the question how accurately the resulting gravitational potential approximates the true one in this galaxy, would require separate studies, which are outside the scope of this paper. Nevertheless, it is still interesting to find out whether the effective surface density, that by construction accounts for the galaxy rotation, would also be consistent with other observational data available for the galaxy. Such a procedure led to consistent results for the galaxy NGC 4736 in (Jalocha et al. 2008) and for the galaxy NGC 5457 in this paper.

Another relation between the rotation velocity and the corresponding surface density is (Toomre 1963)

$$\tilde{\sigma}(\rho) = \frac{1}{\pi^2 G} \mathcal{P} \left[ \int_0^\rho \frac{dv^2(\chi)}{d\chi} \cdot \frac{1}{\rho} K\left(\frac{\chi}{\rho}\right) d\chi + \int_\rho^\infty \frac{dv^2(\chi)}{d\chi} \cdot \frac{1}{\chi} K\left(\frac{\rho}{\chi}\right) d\chi \right], \quad (4)$$

where again  $\mathcal{P}$  denotes a principal value integral. This formula became popular mainly thanks to the handbook by Binney & Tremaine (1987). Provided  $\lim_{\rho \rightarrow 0} v^2(\rho) \rightarrow 0$ , formulas (3) and (4) are equivalent  $\sigma(\rho) \equiv \tilde{\sigma}(\rho)$  unless integration gets cut off at a finite radius. However, the disadvantage in the practical use of the formula (4) is that it contains the first derivative of  $v^2(\rho)$  which is subject to high observa-

tional errors that substantially enlarge the uncertainties in the determination of the surface density.

### 3.1.1 An example

To see how the basic equations of disk model work, we may apply them to the most familiar example provided by the Mestel disk.<sup>3</sup> Let  $\sigma(\rho) = \frac{M}{2\pi a\rho}$  be the disk surface density. On substituting  $\chi = x\rho$  and  $\chi = x^{-1}\rho$ , respectively, in the first and in the second integral in (2), we obtain

$$\frac{v^2(\rho)}{4G\rho} = \frac{M}{2\pi a\rho} \times \left\{ \int_0^1 \frac{(1+x)K(x) - E(x)}{x(1+x)} dx = \frac{\pi}{2} \right\},$$

that is, the rotational velocity is constant:  $v^2(\rho) = \frac{GM}{a}$ . Reversely, for a constant velocity  $v_o = \frac{GM}{a}$ , we obtain from (3), by similar substitutions as before,

$$\sigma(\rho) = \frac{v_o^2}{\pi^2 G\rho} \int_0^1 \frac{(1+x)K(x) - E(x)}{x(1+x)} dx = \frac{v_o^2}{2\pi G\rho} = \frac{M}{2\pi a\rho}.$$

The textbook equation (4) cannot be used for Mestel disk directly, since its rotation curve violates the requirement  $\lim_{\rho \rightarrow 0} v(\rho) = 0$  (otherwise, one would conclude that a disk rotating with constant velocity has vanishing surface density). However, if we write  $v^2(\rho) = v_o^2\Theta(\rho - \varepsilon)$  with small  $\varepsilon > 0$ , where  $\Theta$  stands for the unit step function, then  $v^{2'}(\rho) = v_o^2\delta(\rho - \varepsilon)$ , and now we obtain from (4)  $\sigma(\rho) = \frac{v_o^2 K(\varepsilon/\rho)}{\pi^2 G\rho}$ . In the limit  $\varepsilon \rightarrow 0$  we obtain the correct result  $\sigma(\rho) = \frac{v_o^2}{2\pi G\rho}$  for  $\rho > 0$ , since  $K(0) = \frac{\pi}{2}$ . Again the formula (3) has proved more advantageous than the textbook formula (4).

## 3.2 Some consequences of the nonlocal correspondence between $\sigma$ and $v$

Rotational velocities of disks may attain high values in the regions where the surface mass density decreases rapidly, and can be much larger than rotational velocities of spherically symmetric matter configurations of the same internal mass. To illustrate this, let us consider a sequence of unit mass disks with the surface mass densities

$$\sigma_n(x) = \frac{3+n}{2\pi(n-1)} (2 - (n+1)x^{n-1} + (n-1)x^{n+1}) \Theta(1-x), \quad n > 2. \quad (5)$$

$\Theta$  is the unit step function and  $x$  is a dimensionless radial variable. For  $n$  sufficiently large,  $\sigma_n(x)$ 's are almost constant and fall off rapidly to 0 close to  $x = 1$ . Figure 2 illustrates the surface densities  $\sigma_n(x)$  and the corresponding rotational velocities  $v_n(x)$ . The functional sequence  $v_n(x)$  attains the theoretical limit

$$v_\infty(x) = \begin{cases} \sqrt{\frac{2}{\pi}(K(x) - E(x))}, & 0 < x < 1 \\ \sqrt{\frac{2}{\pi}x(K(x^{-1}) - E(x^{-1}))}, & x > 1 \end{cases},$$

<sup>3</sup> The example is simple but unfortunate since Mestel's disk is incompatible with the mathematical consistency of the disk model, which was referred to in the appendix A, however, by doing calculations carefully, it can be still considered.

which is unbounded at  $x = 1$ . This signals that for large  $n$  and close to  $x = 1$ , the rotational velocity can be much larger than the Keplerian velocity  $v_K(x) = \sqrt{M(x)/x}$ , where  $M(x)$  is the mass function. This simple example illustrates that outside a highly oblate object, where densities are already very small or negligible, the rotation curve may be still non-Keplerian even at distances from the object comparable with its size.

Figure 3 shows another example of a differentially rotating disk. Its rotation curve resembles qualitatively rotation curves of some spiral galaxies. The first maximum in the rotation curve in figure 3(b) reflects the contribution from a central bulge, while the second maximum – from an exponential disk. The outermost data points on this curve would influence mainly the dark matter halo fit. If this model were to represent a real galaxy, the rotation curve could be measured only out to  $x \approx 1$ , since beyond this radius only  $3 \times 10^{-6}$  of the total mass would be present, thus amount hardly detectable. In effect, the total estimated mass predicted by the customary models with dark halos, would be roughly equal to the Keplerian mass evaluated at the cutoff radius – the true mass in this example would be therefore overestimated by a factor of  $\approx 1.7$ .

It is a well known fact, that external spherically symmetric shells of matter do not influence the motions of stars on internal orbits, this is also true when the shells of constant density are homoeoids (Binney & Tremaine 1987). In general, however, the motions of stars are influenced by the presence of external masses. This backward reaction effect is particularly important for disk-like objects. To illustrate this, consider an axisymmetric system composed of a finite disk coplanar with an external massive ring. Figure 4 shows the rotational velocity of test bodies around the center of the system. In the presence of the external ring the velocities are lower than those estimated based on the internal masses only. In the case when the external ring is sufficiently close or massive, such orbits may be impossible (the same is true if the internal mass is spherically symmetric). The presence of external flattened shells of matter may help to explain the very declined parts of rotation curves of some galaxies. It is evident from figure 4 that the rotation of a very oblate system can change much with radius depending on the density gradients. In general, rotational velocities are amplified by negative and attenuated by positive gradients of the disk surface density. The gradients are not less important for the local value of the rotational velocity than the amount of matter.

The elementary facts of disk gravitation discussed above, indicate that mass models of flattened galaxies should be sufficiently general in order to take the disk specific effects into account. An important information about the mass distribution encoded in the rotation curve may be simply overlooked by fitting a too much simplified parametric model, or by assuming the mass density in a luminous galactic subsystem to be proportional to its brightness profile. This in effect may lead to completely different qualitative and quantitative predictions for the same galaxy. A typical example of this situation is provided by the already mentioned galaxy NGC 4736.

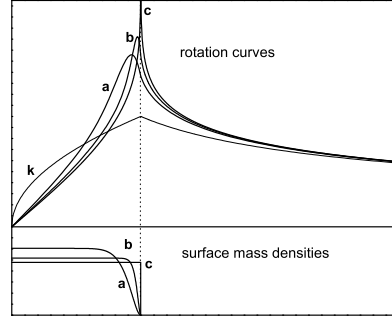


**Figure 2.** The solid lines marked by **a**, **b**, and **c**, show respectively the elements  $n = 16$ ,  $n = 50$ , and the limit  $n \rightarrow \infty$  of the sequence of unit mass disks with the surface mass densities  $\sigma_n$  defined in equation (5), and the corresponding rotational velocities. The rotational velocity in the equatorial plane of a ball with the same mass function as that of the limiting disk is marked by **k**.

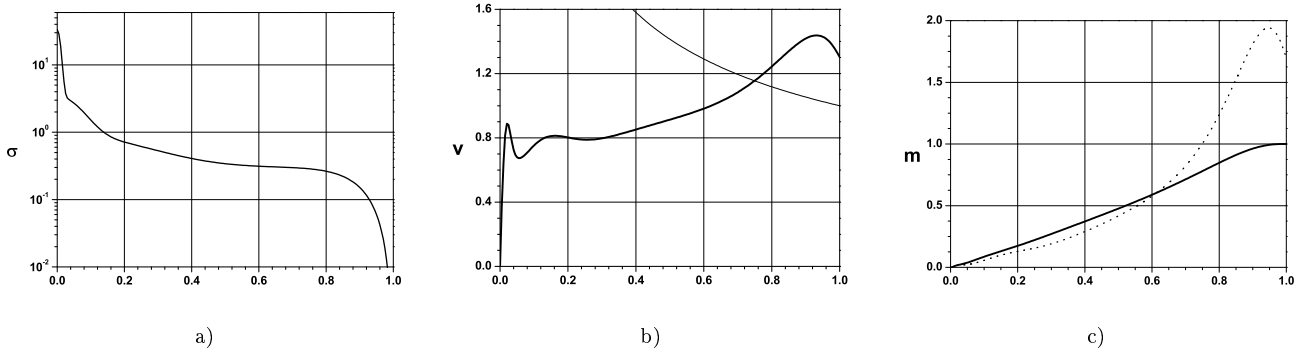


**Figure 3.** **a)** The surface mass density of a unit mass disk:  $\sigma(x) = \frac{100}{51\pi} (48e^{-6400x^2} + 4e^{-400x^2/3} + e^{-100x^2/9}) + \frac{19}{40\pi} (2 - 17x^{15} + 15x^{17}) \Theta(1 - x)$ . **b)** The corresponding rotation curve (thick line) and its Keplerian asymptote (thin line). **c)** The true mass function (solid line) and the Keplerian mass function calculated from the rotation curve (dotted line). Although there is only  $3 \times 10^{-6}$  of the total mass outside the radius  $x = 1$ , the rotation curve is still non-Keplerian and the Keplerian mass is almost twice as big as the true mass. To explain this rotation curve at large radii, one would normally add a massive spherical halo by fitting it into the rising part with the help of the least square method. In this way additional 'missing' mass would be introduced to the system to account for its rotation, while in fact this mass is not present at all.

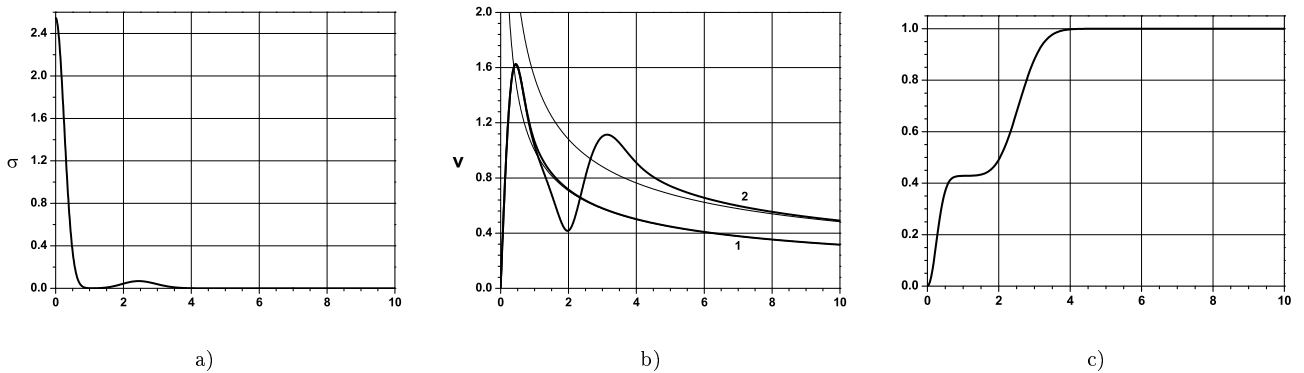


**Figure 4.** The influence of a massive external ring on the value of rotational velocities of test bodies moving on the internal orbits. **a)** The surface mass density of an axisymmetric system composed of an internal disk coplanar with an external ring; **b)** the corresponding rotation curves (and their Keplerian asymptotes) in the situation with (2) and without (1) the external ring; **c)** the mass function. Note, that in the presence of the external ring the rotational velocities in the vicinity of the internal disk are lower than those in the situation without the ring.

#### 4 THE CUTOFF ERROR IN THE DISK MODEL

As follows from equation (3), the mass function of a disk-like system is

$$M(\rho) = \frac{2}{\pi G} \int_0^\rho d\tilde{\rho} \left( \mathcal{P} \int_0^\infty v^2(\tilde{\rho}x) \mathcal{H}(x) dx \right)$$

where

$$\mathcal{H}(x) = \frac{\Theta(1-x)}{x} \left( K(x) - \frac{E(x)}{1-x^2} \right) + \Theta(x-1) \frac{E(x^{-1})}{x^2-1}.$$

The total mass contained within radius  $\rho$  can be therefore determined only when a rotation curve is known globally, whereas the rotation curve of a real galaxy is known only out to a finite distance from its center (we call the distance the cutoff radius). This is the mathematical reason why the surface mass density and the mass function of a flattened galaxy cannot be determined uniquely from the measurements of its rotation curve only. This situation is drastically different from that for a spherically symmetric system in which case the mass function at a given radius is related directly to the local value of rotational velocity:  $M(r) = r v^2(r)/G$ .

Let  $R$  denote the cutoff radius. The integration in (3) gets naturally cut off at  $\rho = R$ , and for  $\rho < R$  we may approximate (3) by

$$\sigma_R(\rho) = \frac{1}{G\pi^2} \mathcal{P} \left[ \int_0^\rho v^2(\chi) \left( \frac{K\left(\frac{\chi}{\rho}\right)}{\rho\chi} - \frac{\rho}{\chi} \frac{E\left(\frac{\chi}{\rho}\right)}{\rho^2 - \chi^2} \right) d\chi + \int_\rho^R v^2(\chi) \frac{E\left(\frac{\rho}{\chi}\right)}{\chi^2 - \rho^2} d\chi \right], \quad \rho < R. \quad (6)$$

Since  $\sigma(\rho) \geq \sigma_R(\rho)$ , expression (6) gives the surface density underestimated with respect to (3) by a cutoff error  $\Delta\sigma_R(\rho) = \sigma(\rho) - \sigma_R(\rho)$ :

$$\Delta\sigma_R(\rho) = \frac{1}{G\pi^2} \int_R^\infty v^2(\chi) \frac{E\left(\frac{\rho}{\chi}\right)}{\chi^2 - \rho^2} d\chi > 0, \quad \rho < R. \quad (7)$$

This error is completely unknown. With the Toomre integral (4) cut off at  $\rho = R$  the situation is even worse. In this case we have for  $\rho < R$

$$\tilde{\sigma}_R(\rho) = \frac{1}{\pi^2 G} \mathcal{P} \left( \int_0^\rho \frac{dv^2(\chi)}{d\chi} \cdot \frac{1}{\rho} K\left(\frac{\chi}{\rho}\right) d\chi + \int_\rho^R \frac{dv^2(\chi)}{d\chi} \cdot \frac{1}{\chi} K\left(\frac{\rho}{\chi}\right) d\chi \right), \quad \rho < R, \quad (8)$$

thus even the sign of the resulting cutoff error  $\Delta\tilde{\sigma}_R(\rho) = \tilde{\sigma}(\rho) - \tilde{\sigma}_R(\rho)$  is unknown, where

$$\Delta\tilde{\sigma}_R(\rho) = \frac{1}{G\pi^2} \int_R^\infty \frac{dv^2(\chi)}{d\chi} \cdot \frac{1}{\chi} K\left(\frac{\rho}{\chi}\right) d\chi, \quad \rho < R, \quad (9)$$

since it depends on a weighted slope of the unknown part of the rotation curve. It should be stressed that although

$\tilde{\sigma}(\rho) \equiv \sigma(\rho)$ , the corresponding cut off integrals are different:  $\sigma_R(\rho) \neq \tilde{\sigma}_R(\rho)$ , thus also different are the cutoff errors,  $\Delta\sigma_R(\rho) \neq \Delta\tilde{\sigma}_R(\rho)$ .

A cutoff error of mass determination of the internal disk of radius  $R$ , and corresponding to  $\Delta\tilde{\sigma}_R$ , reads

$$\Delta\tilde{M}_R = \frac{Rv_R^2}{G} \cdot \frac{2}{\pi} \int_0^1 x dx \int_1^\infty \frac{d\xi}{\xi} \frac{du^2(\xi)}{d\xi} K\left(\frac{x}{\xi}\right),$$

where  $x = \rho/R$ ,  $u(x) = v(xR)/v_R$  and  $v_R = v(R)$ .

Let us consider a theoretical situation of a disk-like galaxy with a rotation curve known to be almost Keplerian outside a cutoff radius  $R$ . One then expects all of the galaxy mass  $M$  to be contained in the disk of radius  $R$ . Then also  $M \approx G^{-1}Rv_R^2$  and  $u(x) \approx 1/\sqrt{x}$  for  $x > 1$ . By using  $\tilde{\sigma}_R(\rho)$  to estimate the mass distribution in this particular situation, we obtain for  $0 < x < 1$

$$\frac{1}{4\pi} < \frac{RG}{v_R^2} \cdot |\Delta\tilde{\sigma}_R(\rho)| = \frac{E(x) - (1-x^2)K(x)}{\pi^2 x^2} < \frac{1}{\pi^2}, \quad (10)$$

thus the resulting total mass is greater by  $|\Delta\tilde{M}_R| = (4/\pi - 1)M \sim 0.27M$  than the actual mass  $M$ . The cutoff error  $|\Delta\tilde{\sigma}_R(\rho)|$  in (10) grows with the distance from the galactic center.

This example leads to the following criterion: provided that most of the disk mass is contained inside a radius  $R$ , the cutoff error is insignificant in the region where  $\tilde{\sigma}_R(\rho)$  satisfies the inequality

$$\tilde{\sigma}_R(\rho) > \frac{1}{\pi^2} \frac{v_R^2}{RG}. \quad (11)$$

Otherwise, the approximation (8) is not reliable, and this occurs at larger radii, close to  $R$ . In the same theoretical situation, the cutoff error corresponding to the integral (6), is given for  $0 < x < 1$  by

$$\frac{RG}{v_R^2} \cdot \Delta\sigma_R(\rho) = \frac{1}{\pi^2} \int_1^\infty \frac{d\xi}{\xi} \frac{E\left(\frac{x}{\xi}\right)}{\xi^2 - x^2}, \quad (12)$$

hence

$$\frac{1}{4\pi} < -\frac{E(x)\ln(1-x^2)}{2\pi^2 x^2} < \frac{RG}{v_R^2} \cdot \Delta\sigma_R(\rho) < -\frac{\ln(1-x^2)}{4\pi x^2},$$

where the inequalities  $1 = E(1) < E(x) < E(x/\xi) < E(0) = \pi/2$  for  $x \in (0, 1)$  and  $\xi > 1$  have been used. The rightmost expression is divergent as  $x \rightarrow 1$ , but for  $x < x_c \approx 0.63$  it is still less than  $\pi^{-2}$ , thus  $\Delta\sigma_R(\rho)$  and  $|\Delta\tilde{\sigma}_R(\rho)|$  are comparable for  $\rho < 0.63R$ . In general, however, nothing is known about the mass distribution beyond  $R$ , therefore the cutoff error can not be even roughly estimated – for if, e.g., outside a cutoff radius  $R$  there existed a ring of dark matter concentric with the disk, like in figure 4, then the error could be arbitrarily large depending on the undetectable annulus' mass.

In figure 5 compared are different approximations of the surface mass density obtained with the help of various methods, for the rotation curve of a model disk with a known mass distribution. To illustrate the influence of the spatial extension of the rotation curve measurements on the accuracy of the reconstruction of the mass distribution, in figure 6 presented is a similar analysis for various samples of the same model rotation curve that was cut off at different radii.

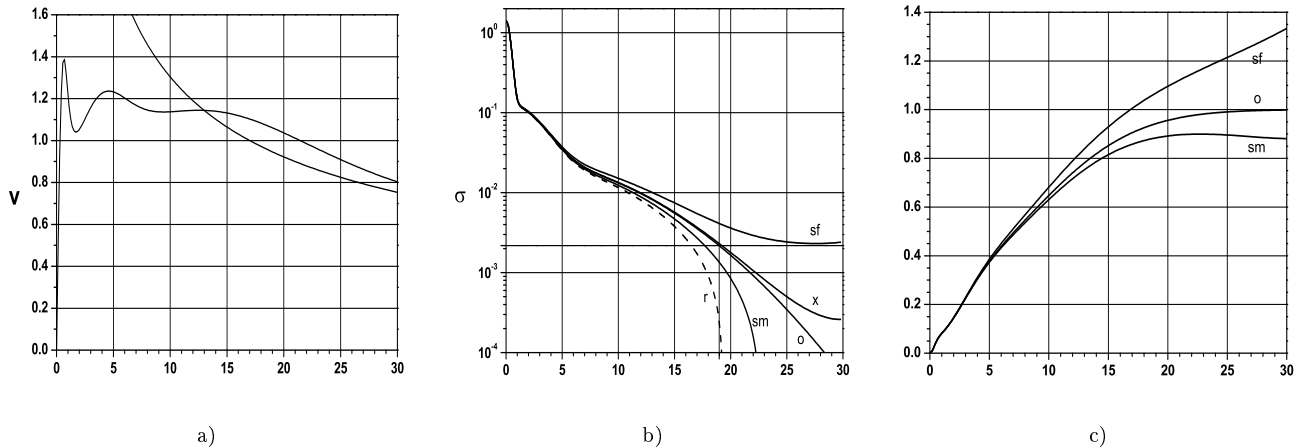


**Figure 5.** **a)** The rotation curve (and its Keplerian asymptote) of a disk with the surface mass density  $\sigma(\rho) = \frac{4}{\pi} \left( e^{-4\rho^2} + \frac{1}{12}e^{-\rho^2/12} + \frac{1}{48}e^{-\rho^2/144} \right)$ . **b)** The surface mass density reconstructed with the help of different methods from the disk's rotation curve cut off at  $R = 30$ : *o* – the exact profile, *sf* – the one calculated from equation (8), *r* – from equation (6), *x* – the *sf* surface density corrected for the contribution from the Keplerian tail according to equation (10), *sm* – the surface density obtained from a spectral representation of the rotation curve (the internal mass was underestimated by 12%) – the surface mass density was calculated in this case from equation (B4). The horizontal line represents the critical value of the surface mass density defined in equation (11), the abscissa of the vertical line is  $\approx 0.63R$ , which is the radius, to which *sf* and *r* may be considered comparable. **c)** The corresponding mass functions.

As follows from the resulting mass functions, the cut off error can be relatively large even in a distant empty region, where the rotation curve is not yet Keplerian, that is, when the cut-off error can not be estimated yet and taken into account. For example, in the surface density diagram in figure 5, the line representing  $\tilde{\sigma}_R(\rho)$  corrected for the cutoff error (10), does not overlap with the exact value of the surface density. Even though 99,9% of the total mass is concentrated in the disk of radius  $R = 30$ , the rotation curve is still not Keplerian outside this radius. At this radius equation (8) overestimates the true mass by 33%, whereas another estimation based on the spectral approximation given in appendix B underestimates the true mass by 12% only.

## 5 MASS-TO-LIGHT RATIO AND THE RESULTS FOR NGC 5457

The mass distribution of the luminous matter in different galaxy subsystems is customarily assumed to be proportional to the corresponding local brightness via constant mass-to-light ratios (frequently the blue band is chosen). This arbitrary assumption ignores the dynamical information about the mass distribution encoded in the non-monotonic features of rotation curves. This in turn, may result in wrong distribution of matter among various galactic components. Especially important are the distant regions where a massive spherical halo is always assumed, whereas in some cases a disk component of baryonic matter may be still more pronounced. The best illustration of this is again the galaxy NGC 4736 (Jalocha at al. 2008). Therefore, it seems better not to correlate the  $M/L$  ratio with the mass distribution and derive it as a point-dependent function from the surface density determined in another way. Then one would be able to trace the presence of different star populations as well as the dark matter distribution.

NGC 5457 (Hubble type Sc I) is one of the largest nearby spiral galaxies, thus also well studied (Bosma at al. 1981). The behavior of the local  $M/L$  ratio for this galaxy inferred from the  $K_s$  band differs from that in the  $B$  band, c.f. figure 7d.<sup>4,5</sup> The reconstruction of the surface mass density strongly depends on the chosen luminosity band – in the most part of NGC 5457, the local  $M/L$  ratio calculated from the  $B$  band is significantly greater than that from the  $K_s$  band. What's more, low-mass, lower temperature stars make up the most of galactic disk. Therefore, the global  $M/L$  ratio in the infrared band, like I, K, i, etc, is the best indicator of the presence of dark matter in spiral galaxies, with  $M/L < 2$  being typical for normal stars.

Although the galaxy NGC 5457 is very large, its rotation curve has been determined only out to 14 kpc (NGC 5457 has an asymmetric Doppler image). The rotation curve breaks the sphericity condition (1), c.f. figure 7, thus, for the reasons discussed in the previous sections, we use the global disk model. To obtain the global mass distribution in this galaxy we applied the method presented in (Jalocha at al. 2008) that combines through iterations the measured rotation curve together with gas measurements far from the galactic center. The method gives a self-consistent global mass distribution in the disk. Self-consistency means that a) the rotation curve calculated from the global surface mass density with the help of integral (2) overlaps with the measured rotation curve, b) the calculated global surface mass density outside the cutoff radius overlaps with the amount of hydrogen and helium visible in the outer parts of this galaxy

<sup>4</sup> These results were reported in part at the XLVII Cracow School of Theoretical Physics in Zakopane (Jalocha at al. 2007).

<sup>5</sup> The measurement data for NGC 5457 were taken from: the  $HI$  surface density & the  $L_B$  luminosity profile (Braun 1997), the galaxy distance (Jarrett), the  $H_2$  surface density (Young 1991), and the rotation curve (Sofue, www page).

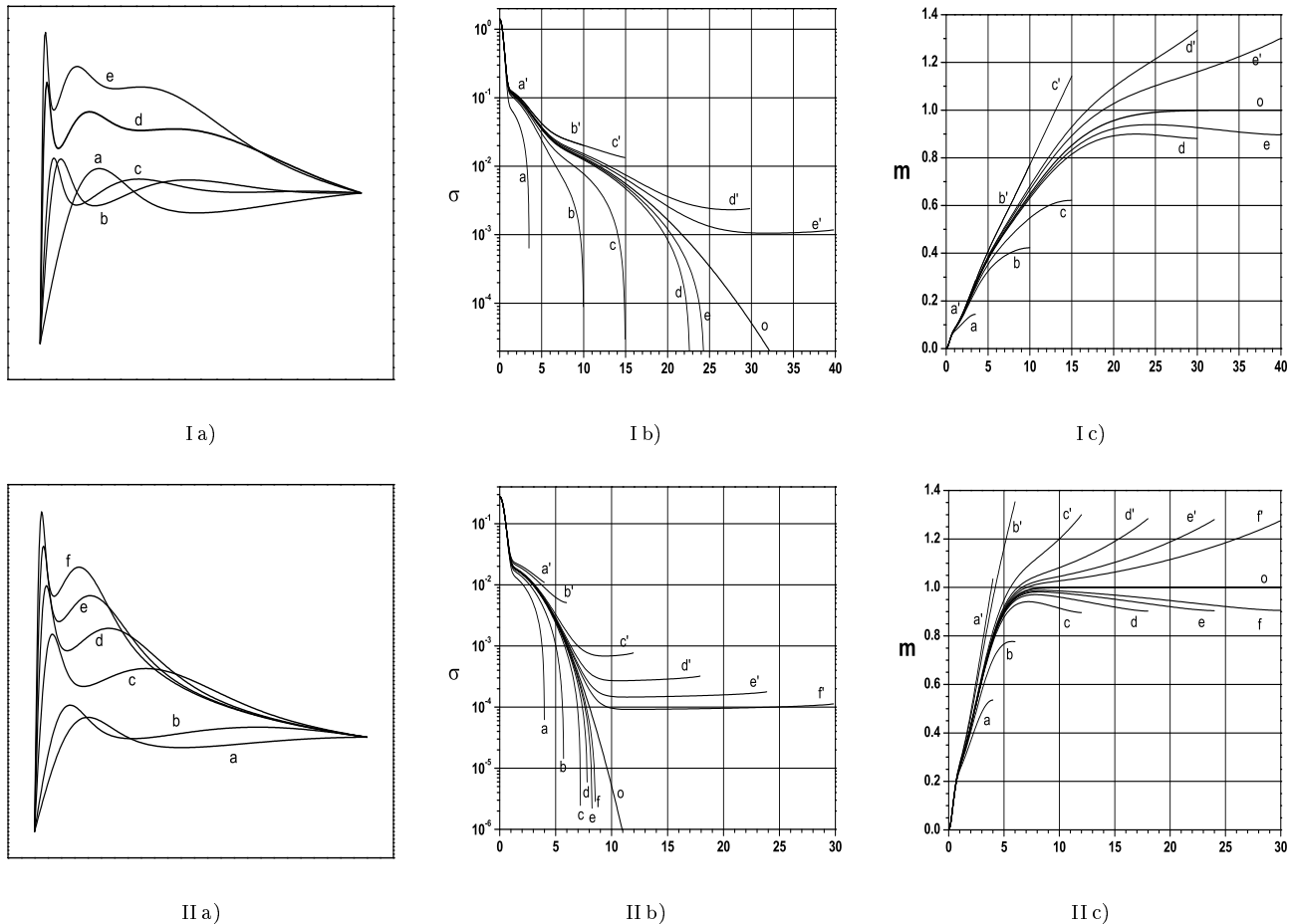


**Figure 6.** The analysis of disk mass distributions which are superpositions of: three gauss profiles discussed in figure 5 (upper plots), and of two exponential profiles (lower plots). The analysis illustrates the influence of the cutoff radius on the accuracy of reconstruction of the original mass distribution. The surface densities were calculated with the help of integral (6) (the lines marked by primed letters) and with the help of the spectral representation (B4) of the rotation curves (the lines without primes). **a)** Various pieces of the corresponding exact rotation curves obtained by cutting off external parts at different radii (the curves are shown in normalized variables  $(x, u)$  explained in the text). **b)** The reconstructed surface mass densities and the original density (denoted by 'o'). **c)** The corresponding mass functions, and the exact asymptotically unit mass function.

and c) the calculated global rotation curve and global surface density are mutual transforms of each other according to integrals (2) and (3).

The global characteristics of the analysis for NGC 5457 are given in table 1. In combination with the observed local brightness  $\lambda$ , the determined surface density  $\sigma$  yields the corresponding local mass-to-light ratio profile  $\sigma/\lambda$ . In the  $K_S$  band,  $\sigma/\lambda$  increases near the disk edge, c.f. figure 7. A similar increase was observed by Sofue for several other galaxies (Takamiya & Sofue 2000). This rise would seem at first as the signature of the presence of dark matter in the outer part of the galaxy. Indeed, if stars were to comprise the whole baryonic mass of the galaxy, the  $\sigma/\lambda$  ratio would be always that of stars, even in the limit  $\lambda \rightarrow 0$ . This is not the case for NGC 5457, however. The increase of the local mass-to-light ratio in this galaxy is caused by the presence of large amounts of hydrogen beyond the stellar disk. If there is some gas, eg. hydrogen and helium, then the local mass-to-light ratio profile  $(\sigma_{stars} + \sigma_{H,He})/\lambda$  diverges as  $\lambda \rightarrow 0$ . But the gas contribution should be subtracted as it is nonlu-

minous in the visible and infrared bands. As is seen in figure 7, after subtraction of the hydrogen and primordial helium contribution, the local mass-to-light ratio profile stops to increase at the disk edge. Also in the  $B$  band the ratio has decreased. This fact, together with the low mass-to-light ratio in the  $K_s$  band, shows that the  $CDM$  halo is not needed to account for this galaxy's rotation. Furthermore, the fact of breaking the sphericity condition, practically excludes a massive and spherical halo of  $CDM$  in NGC 5457.

## 6 CONCLUDING REMARKS

For the accuracy of determination of the mass distribution and its features in the disk component, local non-monotonic properties of rotation curves are important. They are not less important than the value of the rotational velocity. In particular, a local increase in the velocity field may be caused simply by a local decrease of matter density in the disk component and not by the increase of density in the spherical



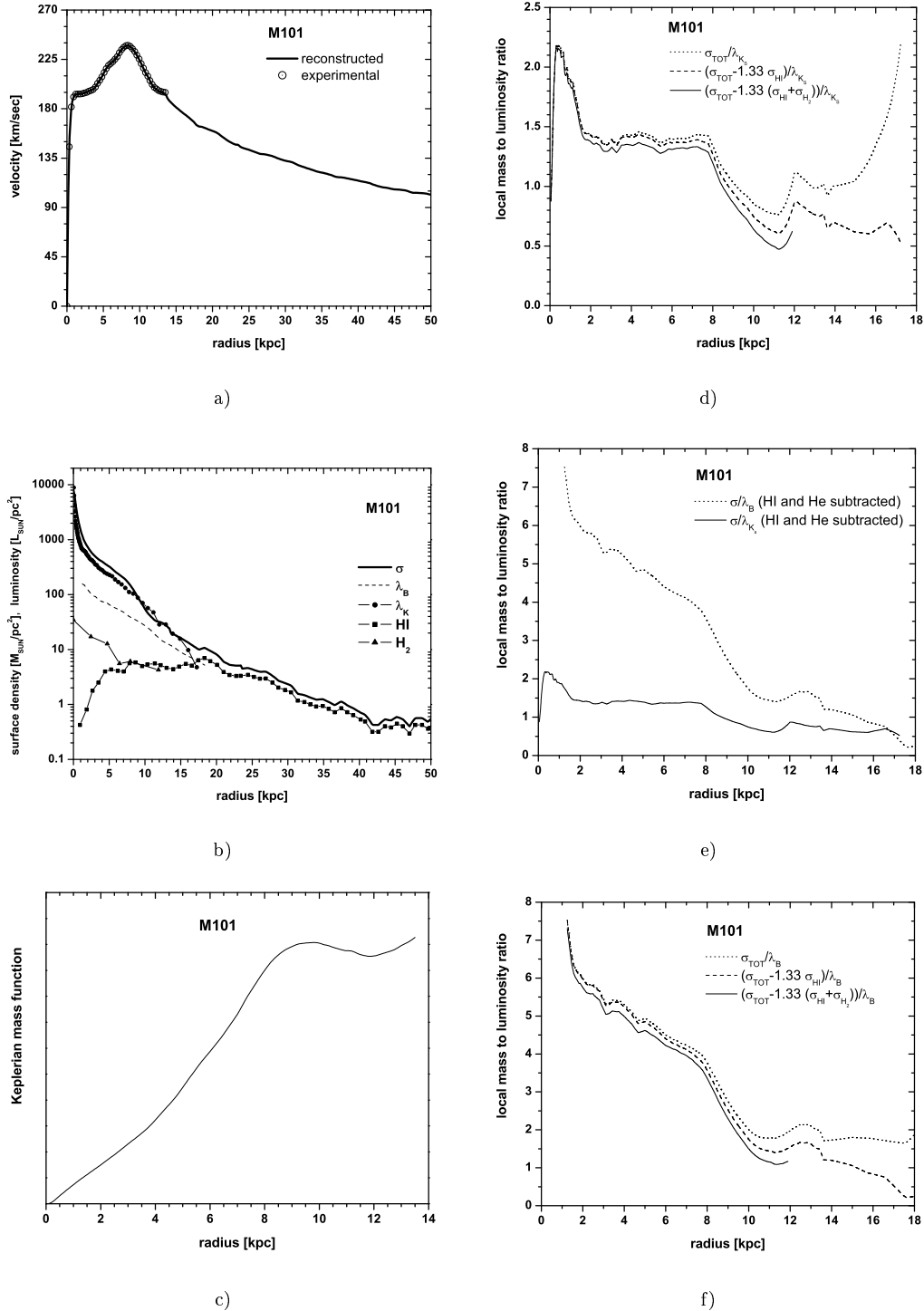


**Figure 7.** The results for spiral galaxy NGC 5457 (M101) obtained in the thin disk model with the use of the iterative method developed in (Jalocha et al. 2008). **a)** the rotation curve calculated from equation (2) for a surface mass density marked by  $\sigma$  in figure b); **b)** the global surface mass density found by applying the iteration method, the hydrogen surface densities for  $HI$ ,  $H_2$ , and the surface luminosity profiles ( $\lambda$ ) (K and B bands); **c)** the Keplerian mass function (11) for the observed part of rotation curve of NGC 5457; **d)** the mass-to-luminosity ratio profile ( $\sigma/\lambda$ ) in  $K_s$  filter for total surface density and with hydrogen  $HI$ ,  $H_2$  and helium subtracted (since they are not seen in the  $K_s$  band); **e)** comparison of local mass-to-luminosity profiles ( $\sigma/\lambda$ ) in  $B$  and  $K_s$  bands (hydrogen and helium subtracted); **f)** the mass-to-luminosity ratio profile in  $B$  filter for the total surface density and the other one with hydrogen  $HI$ ,  $H_2$  and helium subtracted

$M_{TOT}$	$1.13 \times 10^{11} M_{\odot}$
$M_{HI}$	$1.5 \times 10^{10} M_{\odot}$
$M_{H_2}$	$3.4 \times 10^9 M_{\odot}$
$L_{K_S}$	$7.45 \times 10^{10} L_{\odot}$
$L_B$	$2.49 \times 10^{10} L_{\odot}$
$M_{TOT}/L_{K_S}$	1.52
$M_{TOT}/L_B$	4.54
$M_{STAR}/L_{K_S}$	1.27
$M_{STAR}/L_B$	3.8

**Table 1.** The other results for NGC 5457.  $M_{K_S \odot} = 3.45$ ,  $M_{STAR} = M_{TOT} - \frac{4}{3} (M_{HI} + M_{H_2})$ ,  $D = 7.2 \text{Mpc}$ , inclination 18deg

component of a galaxy. The important information about mass distribution carried by rotation curves may be simply overlooked if one assumes that the local mass distribution is proportional to the local brightness. In some cases the dark matter halo is introduced simply because the amount of luminous matter with the constant mass-to-light ratio found by the least square fitting method, cannot account for the rotation at large radii. The example of the spiral galaxy NGC 4736 discussed in (Jałocha et al. 2008) very well illustrates this observation. This shows also that determination of mass distribution in spiral galaxies is model dependent. For more reliable predictions it is thus important to have a generic model, more flexible and general than the parametric models with smooth profiles and constant mass-to-light ratios. It seems that the global thin disk model provides such a generic model, at least for flattened galaxies with rotation curves breaking at large radii the sphericity condition.

Due to observational cutoff in rotation data, the surface mass density reconstruction in the galactic disk (and consequently in the whole galaxy), is subject to high uncertainties, which increase with the distance from the center. Only in particular situations of rotation curves with almost Keplerian tails, the cutoff errors can be eliminated and taken into account. The observationally determined part of a given rotation curve may be explained by various internal disk mass distributions depending on how the rotation law has been extrapolated beyond the cutoff radius. This uncertainty can be removed if additional constraints on the mass distribution in the outer parts, not covered with rotation measurements, are taken into account. In this respect the hydrogen distribution in the outer regions can be used. We have established for galaxies NGC4736 and NGC5457 that the observed amount of baryonic matter accounts for rotation of these galaxies in the approximation of the global disk model.

## References

- Binney, J., Tremaine, S. *Galactic Dynamics*, Princeton Univ. Press, Princeton 1987  
 Bosma A., Goss W.M., Allen R.J. 1981, A&A **93**, 106-112  
 Brandt, J. C. 1960, ApJ **131**, 293  
 Braun, R., 1997, ApJ **484**, 637  
 Burbidge, E. M., Burbidge, G. R., Prendergast, K. H. 1959, ApJ **130**, 739  
 Jałocha, J., Bratek, Ł., Kutschera, M. 2008, ApJ, **679**, 373  
 Jałocha, J., Bratek, Ł., Kutschera, M., Kolonko, M. 2007, Acta Phys. Pol. **B 38**, 3859

Jarrett, T. K-2MASS, NASA/IPAC Informed Science Archive,

<http://irsa.ipac.caltech.edu/date/LGA> LGA

Lebediev, N. N. *Special functions and applications*, Moscow 1953

Ostriker, J. P., Peebles, P. J. E. 1973, ApJ **186**, 467

Ryzhik, I. M., Gradstein, I. S. *Tables of Integrals, sums, series and products*, Moscow, Leningrad, 1951

Sofue, Y. <http://www.ioa.s.u-tokyo.ac.jp/~sofue>

Sofue, Y., and Rubin, V. 2001, ARA&A **39**, 137

Takamiya, T., Sofue, Y. 2000, ApJ **534**, 670

Toomre, A. 1963, ApJ **138**, 385

Toomre, A. 1964, ApJ **139**, 1217

Young, J.S. 1991, ARA&A **29**, 581

## APPENDIX A: BASIC EQUATIONS OF THE AXISYMMETRIC THIN DISK MODEL

We assume an axisymmetric mass distribution over an infinitely thin disk. The cylindrical coordinates  $(\rho, \phi, z)$  are chosen such that the disk overlaps with the  $z = 0$  plane. Gravitational potential  $\Phi$  is  $z$ -symmetric, hence it suffices to consider the half space  $z > 0$ . In this region the complete function space of axisymmetric, everywhere bounded and vanishing at infinity functions is spanned by the base solutions  $J_0(\omega\rho/L)e^{-\omega z/L}$  of the Laplace equation, with  $\omega > 0$  and  $L$  being a length scale. Linearity implies that the most general solution in this function space can be represented as a superposition

$$\Phi(\rho, z) = -2\pi v_L^2 \int_0^{\infty} \hat{\sigma}(\omega) J_0\left(\omega \frac{\rho}{L}\right) \exp\left(-\omega \frac{z}{L}\right) d\omega, \quad (\text{A1})$$

$v_L$  is a velocity scale, and the spectral amplitude  $\hat{\sigma}$  is dimensionless. A dimensionless distance  $x$  and a velocity function  $u(x)$  are defined by

$$x = \frac{\rho}{L}, \quad u(x) = \frac{v(Lx)}{v_L}.$$

The discontinuity of  $\partial_z \Phi$  at  $z = 0$  is interpreted as an infinitely thin layer of mass spread over the disk's plane with the surface mass density

$$\sigma(\rho) = \frac{1}{2\pi G} \partial_z \Phi|_{z=0},$$

hence

$$\sigma(\rho) = \frac{v_L^2}{GL} \cdot \int_0^\infty \omega \hat{\sigma}(\omega) J_0\left(\omega \frac{\rho}{L}\right) d\omega. \quad (\text{A2})$$

Note, that  $\hat{\sigma}(\omega)$  is the spectral amplitude of  $\sigma(\rho)$  (the inverse Hankel transform)

$$\hat{\sigma}(\omega) = \frac{GL}{v_L^2} \int_0^\infty x \sigma(Lx) J_0(\omega x) dx. \quad (\text{A3})$$

The condition for coplanar, circular and concentric orbits in the  $z = 0$  plane reads  $v^2(\rho) = \rho \partial_\rho \Phi(\rho, 0)$  for all  $\rho$ . Hence, having formally differentiated (A1), one gets for  $z = 0$

$$u^2(x) = 2\pi x \int_0^\infty \omega \hat{\sigma}(\omega) J_1(\omega x) d\omega, \quad (\text{A4})$$

and the resulting inverse relation

$$\hat{\sigma}(\omega) = \frac{1}{2\pi} \int_0^\infty u^2(x) J_1(\omega x) dx. \quad (\text{A5})$$

On substituting (A5) to (A2), integrating by parts, provided that  $v(\rho)$  is differentiable, that  $v^2(\rho) \rightarrow 0$  as  $\rho \rightarrow 0$ , that  $v^2(\rho)/\sqrt{\rho} \rightarrow 0$  as  $\rho \rightarrow \infty$ ,<sup>6</sup> and using the upper integral in footnote<sup>7</sup>, we arrive at the Toomre integral

$$\sigma(\rho) = \frac{1}{\pi^2 G} \mathcal{P} \left[ \int_0^\rho \frac{dv^2(\chi)}{d\chi} \cdot \frac{1}{\rho} K\left(\frac{\chi}{\rho}\right) d\chi + \int_\rho^\infty \frac{dv^2(\chi)}{d\chi} \cdot \frac{1}{\chi} K\left(\frac{\rho}{\chi}\right) d\chi \right]. \quad (\text{A6})$$

The integral should be understood in the principal value sense (the symbol  $\mathcal{P}$  indicates this kind of integration), thus the singularity of the elliptic function  $K(y)$  at  $y = 1$  does not contribute. The equivalent form of the Toomre integral (with the same assumptions about  $v(\rho)$  as above) reads

$$\sigma(\rho) = \frac{1}{\pi^2 G} \mathcal{P} \left[ \int_0^\rho v^2(\chi) \left( \frac{K\left(\frac{\chi}{\rho}\right)}{\rho \chi} - \frac{\rho}{\chi} \frac{E\left(\frac{\chi}{\rho}\right)}{\rho^2 - \chi^2} \right) d\chi + \int_\rho^\infty v^2(\chi) \frac{E\left(\frac{\rho}{\chi}\right)}{\chi^2 - \rho^2} d\chi \right]. \quad (\text{A7})$$

<sup>6</sup> These assumptions assure at the same time the existence of integral (A5) and the suitable boundary conditions required for the equivalence of integrals (A6) and (A7) (flat rotation curves are incompatible with these conditions). To assure at the same time mutual invertibility of integrals (A4) and (A5) one needs a stronger condition that  $\lim_{\rho \rightarrow \infty} \sqrt{\rho} v^2(\rho) \rightarrow 0$ .

<sup>7</sup>

$$\int_0^\infty d\omega J_0(\omega x) J_0(\omega \xi) = \begin{cases} \frac{2}{\pi \xi} K\left(\frac{x}{\xi}\right), & 0 < x < \xi \\ \frac{2}{\pi x} K\left(\frac{\xi}{x}\right), & 0 < \xi < x \\ \frac{2}{\pi \xi} \left( K\left(\frac{\xi}{x}\right) - E\left(\frac{\xi}{x}\right) \right), & 0 < \xi < x \\ \frac{2}{\pi x} \left( K\left(\frac{x}{\xi}\right) - E\left(\frac{x}{\xi}\right) \right), & 0 < x < \xi, \end{cases}$$

cf. (Ryzhik & Gradstein 1951).

The integrand has an ordinary pole  $\frac{v^2(\rho)}{2\rho(\chi-\rho)}$  at  $\chi = \rho$ , which is easily integrable numerically and dominates the singularity of the elliptic function  $K$ . The above equation can be derived analogously like the Toomre integral, however it can be also proved by integration by parts the integral (A6) (in order to use the relevant theorems of integral calculus, the integral (A6) should be first rewritten as  $\int_0^{x-\epsilon} + \int_{x+\epsilon}^\infty$ , then integrated by parts, and finally the limit  $\epsilon \rightarrow 0$  should be taken).

The inverse of integral (A7) reads

$$\frac{v^2(\rho)}{4G\rho} = \mathcal{P} \left[ \int_0^\rho \sigma(\chi) \frac{\chi E\left(\frac{\chi}{\rho}\right)}{\rho^2 - \chi^2} d\chi - \int_\rho^\infty \sigma(\chi) \left( \frac{\chi^2 E\left(\frac{\rho}{\chi}\right)}{\rho(\chi^2 - \rho^2)} - \frac{K\left(\frac{\rho}{\chi}\right)}{\rho} \right) d\chi \right]. \quad (\text{A8})$$

Indeed, by substituting (A3) in (A4) one gets

$$\frac{u^2(x)}{x} = 2\pi \int_0^\infty J_1(\omega x) d\omega \left( \frac{GL}{v_L^2} \cdot \int_0^\infty \sigma(Ly) \partial_y (y J_1(\omega y)) dy \right)$$

where the identity  $\omega^{-1} \partial_y (y J_1(\omega y)) = y J_0(\omega y)$  has been used. Next, on integrating by parts, with the assumption that  $\rho^2 \sigma(\rho) \rightarrow 0$  as  $\rho \rightarrow 0$  and  $\sqrt{\rho} \sigma(\rho) \rightarrow 0$  as  $\rho \rightarrow \infty$ , we obtain

$$\frac{u^2(x)}{x} = \frac{GL}{v_L^2} \left( -2\pi \int_0^\infty \xi d\xi \partial_\xi \sigma(L\xi) \int_0^\infty J_1(\omega \xi) J_1(\omega x) d\omega \right).$$

The rightmost integral is given in footnote<sup>7</sup>. On integrating by parts again, with the same assumptions about the limiting behavior of  $\sigma(\rho)$  as before, one arrives at the final result (A8). When doing these calculations, the same integration splitting and taking the limit, as in the derivation of (A7), applies.

A simple analytic example using the above formulas and illustrating the equivalence of (A6) and (A7) was given in section 3.1.1.

## APPENDIX B: A DISCRETE SPECTRAL REPRESENTATION

For the observational reasons, a rotation curve  $v(\rho)$  of a galaxy is known only for radii  $\rho \in (0, R)$ ,  $R$  is the data cutoff radius. Let's define  $x = \rho/R$ ,  $u(x) = v(Rx)/v_R$  with  $v_R \equiv v(R)$ . The function  $u^2(x)/x$  is thus defined on the unit interval  $x \in (0, 1)$  and  $u(1) = 1$ . Under some assumptions the function  $u^2(x)/x$  can be represented in this interval as a series of a complete set of orthogonal functions on this interval. Although we may choose any complete set of functions satisfying the appropriate boundary conditions on this interval, best suited for the disk symmetry are cylindrical functions. If  $u^2(x)/\sqrt{x}$  is integrable in the interval  $x \in (0, 1)$  then  $u^2(x)/x$  can be represented in this interval as a series of Bessel functions (Lebediev 1953). To conform with the more general integral representation (A4) we choose the Bessel function of the first order, then

$$\frac{u^2(x)}{x} = \sum_k \check{\sigma}_k J_1(\omega_k x), \quad 0 < x < 1, \quad J_0(\omega_k) = 0. \quad (\text{B1})$$

The summation is taken over all positive zeros  $\omega_k$  of the Bessel function of the zeroth order  $J_0(x)$ . On multiplying both sides by  $x J_1(\omega_m x)$  and integrating over  $x \in (0, 1)$  one gets

$$\check{\sigma}_k = \frac{\omega_k}{J_1(\omega_k)} \mu_k, \quad \mu_k = \frac{2}{\omega_k} \int_0^1 u^2(x) \frac{J_1(\omega_k x)}{J_1(\omega_k)} dx. \quad (\text{B2})$$

The countable set of  $\check{\sigma}_k$ 's suffices to describe  $v(\rho)$  completely only for  $\rho < R$ . However, this information is insufficient to obtain the continuous spectrum  $\hat{\sigma}(\omega)$  of the true global  $\sigma(\rho)$ , thus even for  $\rho < R$  one is unable to determine  $\sigma(\rho)$  from the observed part of rotation curve. This can be done only approximately. For example, assuming that  $v(\rho) = 0$  for  $\rho > R$ , we obtain from (A5)

$$\hat{\sigma}(\omega) = \frac{1}{2\pi} \sum_k \check{\sigma}_k \frac{\omega J_0(\omega) J_1(\omega_k)}{\omega_k^2 - \omega^2}.$$

Since  $J_0(\omega) \approx J_1(\omega_k)(\omega_k - \omega)$  when  $\omega \approx \omega_k$ , the spectrum is continuous. Another extension of  $v(\rho)$  beyond  $R$  arises by assuming that expansion (B1) is formally valid also for  $\rho > R$ , then we obtain from (A5) a discrete spectrum

$$\hat{\sigma}(\omega) = \frac{1}{2\pi} \sum_k \check{\sigma}_k \frac{\delta(\omega - \omega_k)}{\omega}. \quad (\text{B3})$$

It should be clear, that in a similar way, one can construct from the  $\check{\sigma}_k$ 's set, infinitely many other spectra  $\hat{\sigma}(\omega)$ . They will correspond to different global surface densities giving the same rotation law for  $\rho < R$  and different for  $\rho > R$ . In particular, this is the case for the global surface mass densities obtained by taking the inverse transform of the above two spectra.<sup>8</sup> However, the closer to the galactic center the less the two mass distributions differ from each other. Indeed, the error of determining  $\sigma$ , which is calculated from equation (9) in the limit of small radii, reads

$$\lim_{\rho \rightarrow 0} \Delta \tilde{\sigma}_R(\rho) = \frac{v_R^2}{RG} \cdot \frac{1}{2\pi} \int_1^\infty d\xi \frac{u^2(\xi) - 1}{\xi^2}, \quad u(1) = 1,$$

thus should be much smaller than the characteristic density scale  $v_R^2/(RG)$  (as was shown in section 4 it is about 8% of the scale for Keplerian falloff), while the central density is usually much greater than this scale.

With this  $\hat{\sigma}(\omega)$  we obtain from (A2) the following series

<sup>8</sup> The fact that a function defined on the whole real axis, when restricted to a finite interval can be represented by many discrete and continuum spectra, should not astonish. To give a simple example, consider a function such that  $f(x) = \sin x$  for  $x \in (0, \pi)$  and  $f(x) = 0$  elsewhere. Then

$$\hat{f}(\omega) = \frac{1 + e^{-i\pi\omega}}{2\pi(1 - \omega^2)} \quad \text{and} \quad \hat{f}(\omega) = \frac{1}{i} \delta(\omega^2 - 1)$$

are distinct spectral representations of this function on the interval  $(0, \pi)$ , that is, the inverse transform  $\int_{-\infty}^{+\infty} \hat{f}(\omega) e^{i\omega x} d\omega$  converges to  $\sin(x)$  in this interval for both the spectra. Note, however, that outside the interval the integral converges to different functions.

$$\Sigma(\rho) = \frac{v_R^2}{GR} \cdot \frac{1}{2\pi} \sum_k \check{\sigma}_k J_0(\omega_k x), \quad x = \frac{\rho}{R} < 1, \quad (\text{B4})$$

where  $\check{\sigma}_k$ 's have been calculated with the help of (B2). Let  $\rho_1 > 0$  be the smallest radius at which  $\Sigma(\rho)$  becomes negative. By definition one sets in this approximation of the true  $\sigma(\rho)$  that  $\sigma(\rho) \approx \sigma_A(\rho)$  where  $\sigma_A(\rho) = 0$  for  $\rho > \min(\rho_1, R)$ , and  $\sigma_A(\rho) = \Sigma(\rho)$  for  $0 < \rho < \min(\rho_1, R)$ . Then close to the center, the integral (A8) with  $\sigma(\rho) = \sigma_A(\rho)$ , quite well approximates the original rotation curve that was cut off at  $R$  (c.f. section 4 for more details).